Microstrip Open-End and Gap Discontinuities in a Substrate–Superstrate Structure

HUNG-YU YANG, MEMBER, IEEE, NICOLAOS G. ALEXOPOULOS, FELLOW, IEEE, AND DAVID R. JACKSON, MEMBER, IEEE

Abstract—**Overlays (superstrates) are of practical use in a variety of microstrip circuit applications. This article presents the analysis and modeling of microstrip open-end and gap discontinuities in a substrate–superstrate structure using the numerical solution of integral equations. Good accuracy is achieved by adopting semi-infinite and subdomain mode expansion functions, with a transverse coordinate dependence obtained from a two-dimensional infinite line analysis. A parametric study of the material layer effects on radiation and surface wave losses and of the fringing fields at the discontinuities is also performed.**

I. INTRODUCTION

MICROSTRIP open-end and gap discontinuities are useful in the design of matching stubs and coupled filters. In recent years, layered integrated structures have found various applications in MIC's, especially for monolithic integration. Therefore, design data for open-end and gap discontinuities in layered structures would be useful. In this paper, microstrip open-end and gap discontinuities in a substrate–superstrate configuration (Fig. 1) will be considered. The characterization of these discontinuities for a single layer has been performed quite extensively in the past. Quasi-static analysis based on solving Laplace's equation has been applied for low-frequency applications [1]–[4]. For higher frequencies, models based on rigorous dynamic analysis are required. Frequency-dependent results in shielded microstrip structures have been presented [5]–[8]. A dynamic method based on solving integral equations by the method of moments has recently been applied to the modeling of microstrip open-end and gap discontinuities for a single layer case [9], [10]. This analysis takes into account all the physical effects, among them radiation, surface waves, and dominant as well as higher order mode coupling. In [9] a finite but long microstrip line with a δ gap source is used, which typically requires many basis functions and may be numerically inefficient. In [10] a more efficient method, using a combination of the entire domain modes and subdomain modes, is used. However, from the discussion presented in [10], it appears that an improvement is needed for the capacitance calculation.

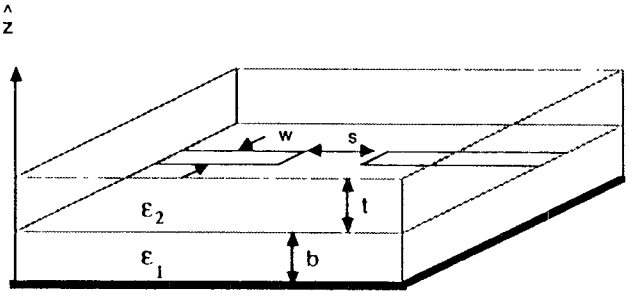

Fig. 1. Microstrip open end and gap in a two-layer structure: $h = t + b$.

A crucial step in the method of moments is to choose suitable expansion functions to provide efficient and accurate numerical computation. A combination of semi-infinite traveling-waves modes and local subdomain modes is fruitful and can be modified easily to adapt to different geometries. The traveling-wave mode corresponds to the fundamental guided-wave mode of the microstrip line. The local subdomain modes are used in the vicinity of the discontinuity region to take into account the higher order mode effects. For the transverse dependence of the expansion functions, it is possible that for sufficiently high frequencies, the simple Maxwellian or pulse function may not be a good approximation when the dominant mode is not TEM-like. Therefore in this analysis, the transverse dependence of the longitudinal current is obtained by a two-dimensional infinite line analysis where three modified cosine Maxwellian functions are used. The characterization of an open-end discontinuity is through the open-end capacitance, which is mainly due to the fringing electric fields, or excess length. When radiation and surface wave losses are considered, a conductance should also be included in the equivalent circuit model. The gap discontinuity is usually modeled as a π network with two capacitances as shown in Fig. 2. The loss mechanism can also be included by adding the two conductances in Fig. 2. The material effects of the layered structure on the radiation and surface wave loss, together with the fringing fields at the discontinuities, will also be discussed.

Manuscript received November 27, 1988; revised April 3, 1989. This work was supported by the U.S. Army Research Office under Contract DAAG 03-83-0090.

H.-Y. Yang was with the Electrical Engineering Department, University of California, Los Angeles, CA 90024. He is now with Phraxos Research and Development, Inc., 2716 Ocean Park Blvd., Santa Monica, CA 90405.

N. G. Alexopoulos is with the Electrical Engineering Department, University of California, Los Angeles, CA 90024-1594.

D. R. Jackson is with the Electrical Engineering Department, University of Houston, University Park, TX 70005.

IEEE Log Number 8929903.

0018-9480/89/1000-1542$01.00

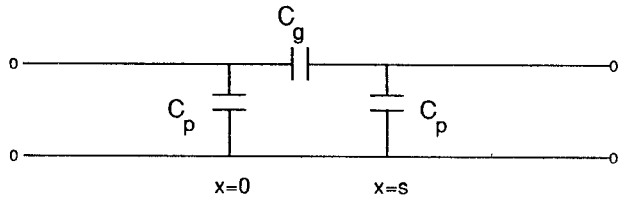

Fig. 2. Equivalent circuit of a microstrip gap.

II. The Method of Moments and Matrix Formulation

If only the longitudinal current in the microstrip line is considered, the integral equation for the open-end case can be written in terms of the longitudinal electric field on the microstrip only as

$$E_x(x, y, z) = \int_{-\infty}^{0}\int_{-w/2}^{w/2} G_{xx}(x, y, z|x_s, y_s, z_s) \cdot J_x(x_s, y_s)\, dy_s\, dx_s = 0 \quad (1)$$

where E_x is the electric field due to the current at $z = z_s$. The Green's function G_{xx} is the value of E_x at the (x, y) point of the microstrip due to an $\hat{x}$-directed delta function at (x_s, y_s). This Green's function has been described [11]. Since the microstrip open end is a special case of the gap discontinuity, the formulation will be for the gap case. The current in the microstrip gap can be expanded as

$$J_x(x, y) = f(x)J_t(y) \quad (2)$$

with

$$f(x) = e^{-jk_m x} - \Gamma e^{jk_m x} + \sum_{n=1}^{N} I_{n1} f_n(x) \qquad \text{for } x \leqslant 0 \quad (3)$$

$$f(x) = Te^{-jk_m(x-s)} + \sum_{n=1}^{N} I_{n2} g_n(x) \qquad \text{for } x \geqslant s \quad (4)$$

and

$$J_t(y) = \frac{a_0 + a_1 \cos\left(\frac{2\pi}{w}y\right) + a_2 \cos\left(\frac{4\pi}{w}y\right)}{\pi w\sqrt{1-(2y/w)^2}} \quad (5)$$

where Γ is the reflection coefficient from the discontinuity and T is the wave amplitude of the transmitted wave. The parameters k_m, a_0, a_1, and a_2 are obtained through an infinite line analysis, which involves solving a characteristic equation in a matrix form [12]. The piecewise-sinusoidal (PWS) modes are defined in [9].

When the expansion functions are used in (1), followed by a nearly Galerkin procedure [10], integral equations are converted into a set of linear equations. These $2N+2$ equations, when expressed in matrix form, are

$$\begin{bmatrix} [Z_{\text{self}}] & [Z_{t\,\text{self}}] & [Z_{ee\,\text{act}}] & [Z_{te\,\text{act}}] \\ [Z_{ee\,\text{act}}] & [Z_{te\,\text{act}}] & [Z_{\text{self}}] & [Z_{t\,\text{self}}] \end{bmatrix} \begin{bmatrix} [I_1] \\ \Gamma \\ [I_2] \\ T \end{bmatrix} = \begin{bmatrix} [I_{\text{inc}_1}] \\ [I_{\text{inc}_2}] \end{bmatrix}. \quad (6)$$

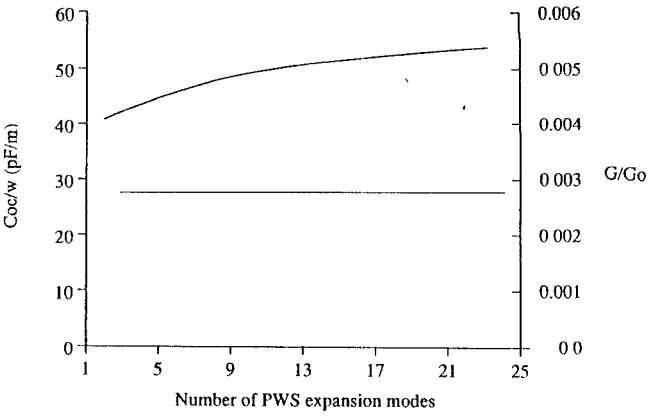

Fig. 3. Convergence test for open-end circuit parameters: $\epsilon_1 = 9.6$, $b = 0.02\lambda_0$ and $w/b = 1$.

The matrix elements in each submatrix are in the form of double infinite integration, for example,

$$Z_{\text{self}}^{nm} = \int_{-\infty}^{\infty}\int_{-\infty}^{\infty} \bar{G}_{xx}(\lambda_x, \lambda_y) F_1^2(\lambda_y) A_1^2(\lambda_x) \cdot \cos\left[\lambda_x(m-n)d_1\right] d\lambda_x\, d\lambda_y \quad (7)$$

where $A_1(\lambda_x)$ and $F_1(\lambda_y)$ are the Fourier transforms of the expansion functions in the $\hat{x}$ and $\hat{y}$ directions respectively. Numerical methods for the computation of (7) were discussed in detail in [11] and [13].

III. Discussion of the Results

Usually MIC discontinuities are characterized by their equivalent circuits. Therefore, in order for the characterization to be meaningful, all the higher order modes causing distortion from the quasi-TEM current should quickly die out as one moves away from the discontinuity. In microstrip structures, any discontinuity will generate radiating and surface waves. When radiating or surface wave fields are strong enough such that their interactions with the microstrip guided mode become significant far from the discontinuity, the computed equivalent circuits will not be accurate. In other words, the results will be different at different reference planes. This phenomenon limits the possible operating frequency of the devices.

The equivalent circuit of a microstrip open end is computed from the reflection coefficient which is obtained directly from the matrix solution of (6). The convergence of the results depends on the size of both the expansion functions and the region where the subdomain modes are used. An example of a convergence check for the open-end conductance and capacitance is shown in Fig. 3. This check is carried out by varying the number of modes used in a fixed subdomain mode region. The subdomain region is chosen as ten times the substrate thickness. It is found that with only two modes, a convergent result for the conductance calculation has already occurred. However, the convergence of the capacitance value is very slow with respect to the number of expansion modes. The region where the subdomain modes are used is less important. It is found that the results are almost unchanged by changing the covered range of the subdomain modes. Physically, this

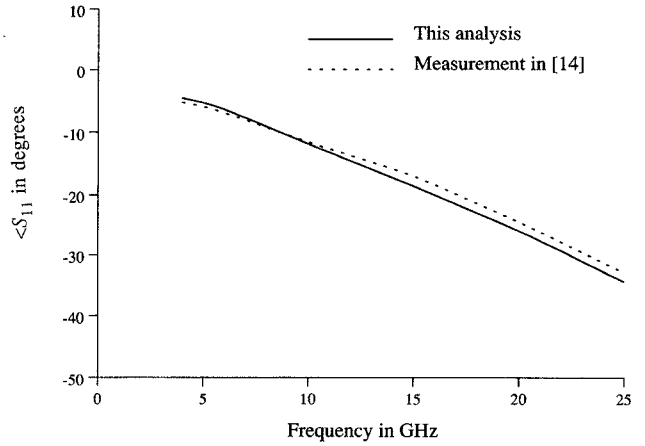

Fig. 4. Theoretical and measured phase of S_{11} for a microstrip open end: $\epsilon_r = 9.9$, $h = 0.635$ mm, and $w = 0.95h$.

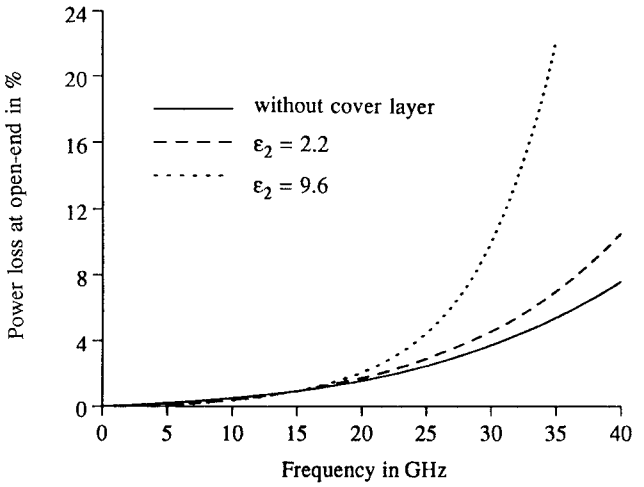

Fig. 5. Energy loss at microstrip open end versus frequency: $\epsilon_1 = 9.6$, $b = 0.3$ mm, $w = b$, and $t = b$.

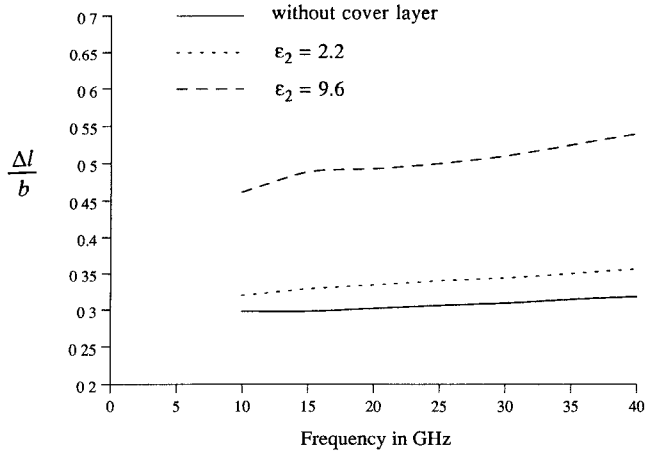

Fig. 6. Excess length of an open-end microstrip versus frequency: $\epsilon_1 = 9.6$, $b = 0.3$ mm, $w = b$, and $t = b$.

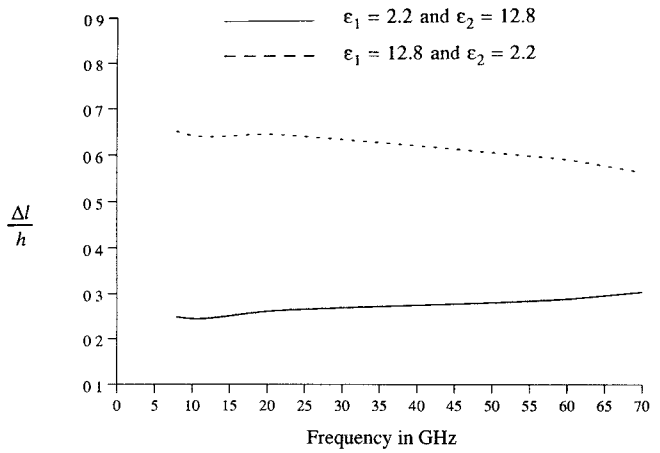

Fig. 7. Excess length of an open-end microstrip versus frequency: $b = t = h/2$, $h = 0.3$ mm, and $w/h = 1$. Microstrip is at the air–dielectric interface.

means that the higher order modes generated by the discontinuity have already died out in the testing region. The above convergence tests are for the case where the radiating and surface waves are weakly excited. It is found that the results will not be as good when the surface waves and radiation loss are strong, due to their interaction with the microstrip fundamental mode. For a circuit to be useful, radiation and surface wave loss should be as small as possible. With a careful convergence study, it is found that, within the useful frequency range, typically 19 PWS modes of size 0.06 guided wavelength can provide results within a few percent accuracy. The validity of the current analysis has been checked against the quasi-static method [4] at low frequencies, with excellent agreement. The theoretical results for the phase of S_{11} of the open end are compared against the measured results presented in [14] and the comparisons are shown in Fig. 4. It is found that the difference between the theory and measurement is less than 1° over the frequency range of the measurement.

Energy loss due to radiation and surface waves at a microstrip open end is shown in Fig. 5 with and without a cover layer. The microstrip line in this case is embedded between the substrate and the superstrate. It is found that with the presence of the cover layer, the loss increases with the increase of the superstrate dielectric constant due to stronger radiation and surface waves. The length extension (or capacitance) at the open end due to the fringing field for the same geometry as that in Fig. 5 is shown in Fig. 6. It is found that by adding a cover layer the excess length to substrate thickness ratio (or end capacitance) is larger due to a stronger fringing field. In general, the excess length increases with the increase of effective dielectric constant and is insensitive to frequency, except when the surface waves are strong. The excess length values for microstrip in a composite substrate (microstrip is at the air–dielectric interface) are shown in Fig. 7. Two different material arrangements were investigated, which include the case of a large permittivity on the top with a lower one on the bottom and vice versa. It is found that the excess length value for the first case is significantly larger than the second one. This implies that, when the microstrip line is on the larger dielectric constant material, the fringing electric field is stronger. It is also interesting to see that for the composite structure, the results are more frequency

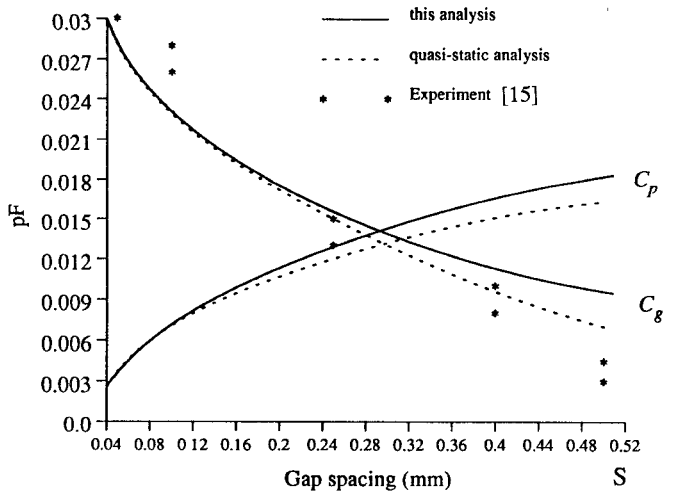

Fig. 8. Gap capacitances versus gap spacing: $\epsilon_1 = 8.875$, $\epsilon_2 = 1$, $b = 0.508$ mm, and $w = b$.

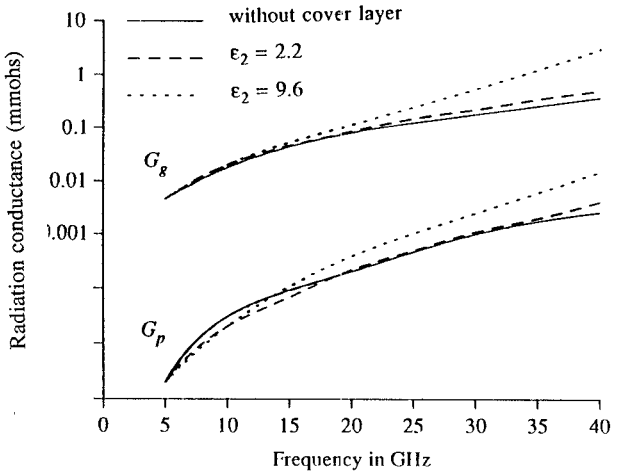

Fig. 9. Gap conductance versus frequency: $\epsilon_1 = 9.6$, $b = 0.3$ mm, $w = b$, $t = b$, and $s = 0.3762b$. Note the nonlinear scale.

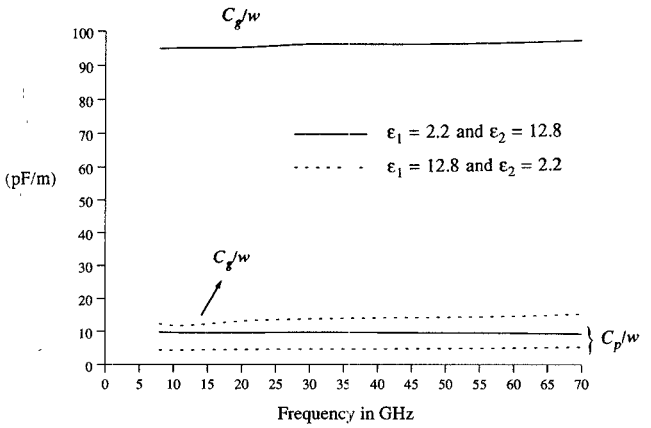

Fig. 10. Normalized gap capacitance versus frequency: $b = t = h/2$, $h = 0.3$ mm, $s = 0.2\ h$, and $w/h = 1$. Microstrip is at the air–dielectric interface.

dependent, which is due to the fact that the dominant mode is less TEM-like.

For the gap case, the reflection coefficients Γ and the transmission coefficient T are S_{11} and $-S_{12}$ respectively. Therefore, the admittance matrix of the gap discontinuities can be obtained by the following transformation:

$$[Y] = ([U]-[S])([U]+[S])^{-1} \tag{8}$$

where $[U]$ is the identity matrix. By comparing the two-port π network and Fig. 1, one has

$$\frac{G_p + j\omega C_p}{G_0} = Y_{11} - Y_{12} \tag{9}$$

and

$$\frac{G_g + j\omega C_g}{G_0} = Y_{12}. \tag{10}$$

The results for the gap discontinuity are first compared with those obtained by the quasi-static method [2] and those obtained by measurements [15], with the result shown in Fig. 8. In this analysis, the frequency is chosen to be 5 GHz. Since the gap capacitance is small and is sensitive to the device tolerances, this type of measurement is inherently difficult to perform accurately. It is found that this dynamic model agrees well with the quasi-static approach. Some discrepancies for large gap spacing may be due to the fact that, in such cases, the amount of energy coupled through the gap is comparable to the energy losses due to surface waves and radiation, and this aspect is not included in the quasi-static approach. This would tend to explain the larger value of C_g obtained with the dynamic approach. The gap conductances G_p and G_g are shown in Fig. 9 for the same material arrangements as those shown in Fig. 5. It is found that the cover layer (superstrate) will increase conductance due to a stronger fringing field and a greater energy losses. Also since $G_p + j\omega C_p$ represents the input admittance when a perfect magnetic wall is in the middle of the gap, it is expected that, due to image cancellation, G_g will be much larger than G_p. As shown in Fig. 9, G_g is about two orders of magnitude larger that G_p. For a narrower gap, C_g will be larger than C_p due to stronger end coupling. However for wide gap spacing, the input admittance seen from either side of the gap is mainly the open-end admittance, so C_p will be larger than C_g. The results for the microstrip gap on top of the superstrate are shown in Fig. 10. It is found that C_g/w is more frequency dependent than C_p/w when the dispersion is strong and that both capacitances are sensitive to frequency when the high-permittivity layer is the one close to the line.

IV. Conclusion

In this paper, we presented the results of microstrip open-end and gap discontinuities in a two-layer structure. The importance of the cover layer effect is also addressed. The accuracy of the results has been checked, in a limiting case, with excellent agreement with the quasi-static solutions.

References

[1] K. C. Gupta, R. Garg and I. J. Bahl, *Microstrip Lines and Slotlines*. Dedham, MA: Artech House, 1979.

[2] M. Maeda, "Analysis of gap in microstrip transmission lines," *IEEE Trans. Microwave Theory Tech.*, vol. MTT-20, pp. 390–396, June 1972.
[3] P. Benedek and P. Silvester, "Equivalent capacitance for microstrip gap and steps," *IEEE Trans. Microwave Theory Tech.*, vol. MTT-20, pp. 729–733, Nov. 1972.
[4] P. Benedek and P. Silvester, "Equivalent capacitance for microstrip open circuit," *IEEE Trans. Microwave Theory Tech.*, vol. MTT-20, pp. 511–516, May 1972.
[5] E. Hammerstad, "Computer-aided design of microstrip couplers with accurate discontinuity models," in *IEEE MTT-S Int. Microwave Symp. Dig.*, 1981, pp. 54–56.
[6] R. H. Jansen, "Hybrid-mode analysis of end effects of planar microwave and millimeterwave transmission line," *Proc. Inst. Elec. Eng.*, pt. H, vol. 128, pp. 77–86, 1981.
[7] N. H. L. Koster, R. H. Jansen and M. Kirschning, "Accurate model for the open end effect of microstrip line," *Electron. Lett.*, vol. 17, pp. 532–535, 1981.
[8] J. S. Hornsby, "Full-wave analysis of microstrip resonator and open circuit end effect," *Proc. Inst. Elec. Eng.*, pt. H, vol. 129, pp. 338–341, 1982.
[9] P. B. Katehi and N. G. Alexopoulos, "Frequency-dependent characteristics of microstrip discontinuities in millimeter wave integrated circuits," *IEEE Trans. Microwave Theory Tech.*, vol. MTT-33, pp. 1029–1035, Oct. 1985.
[10] R. W. Jackson and D. M. Pozar, "Full wave analysis of microstrip open-end and gap discontinuities," *IEEE Trans. Microwave Theory Tech.*, vol. MTT-33, pp. 1036–1042, Oct. 1985.
[11] H. Y. Yang and N. G. Alexopoulos, "Basic block for high frequency interconnects: Theory and experiment," *IEEE Trans. Microwave Theory Tech.*, vol. 36, pp. 1204–1211, Aug. 1988.
[12] O. Fordham, "Two layer microstrip transmission lines," Master's thesis, UCLA, 1987.
[13] H. Y. Yang, "Frequency dependent modeling of passive integrated circuit components," Ph.D. dissertation, UCLA, 1988.
[14] G. Gronau and I. Wolff, "A simple broad-band device DE-embedding method using an automatic network analyzer with time-domain option," *IEEE Trans. Microwave Theory Tech.*, vol. 37, pp. 479–483, Mar. 1989.
[15] *The Microwave Engineer's Handbook and Buyers' Guide*. New York: Horizon House, 1969, p. 72.

Hung-Yu Yang (S'87–M'88) was born in Taipei, Taiwan, on October 25, 1960. He received the B.S. degree in electrical engineering from National Taiwan University in 1982 and the M.S. and Ph.D. degrees from the University of California at Los Angeles in 1985 and 1988, respectively.

Since 1988 he has been with Phraxos Research and Development Inc., Santa Monica, CA, as a research engineer in charge of the development of CAD for passive integrated circuit components in the millimeter-wave range, the development of printed antenna array technology, and the modeling of frequency selective surfaces.

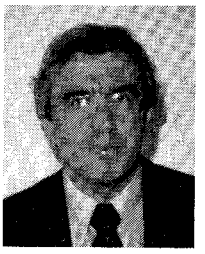

Nicolaos G. Alexopoulos (S'68–M'69–SM'82–F'87) graduated from the 8th Gymnasium of Athens, Greece, and received the B.S.E.E., M.S.E.E., and Ph.D. degrees from the University of Michigan, Ann Arbor, in 1964, 1967, and 1968, respectively.

Currently he is Professor and Chairman of the Electrical Engineering Department at the University of California, Los Angeles. He is also a Consultant with Northrop Corporation's Advanced Systems Division. His current research interests are in electromagnetic theory as it applies to the modeling of integrated-circuit components and printed circuit antennas for microwave and millimeter-wave applications, substrate materials and their effect on integrated-circuit structures and printed antennas, integrated-circuit antenna arrays, and antenna scattering studies. He is also interested in the interaction of electromagnetic waves with materials, in particular, active media.

Dr. Alexopoulos is an Associate Editor of the journals *Electromagnetics* and *Alta Frequenza* and is on the Editorial Boards of the IEEE TRANSACTIONS ON MICROWAVE THEORY AND TECHNIQUES and the *International Journal on Electromagnetics Theory*. He served as the 1974 Chairman of the IEEE APS Chapter. He was a corecipient (Honorable Mention) of the 1983 AP-S R.W.P. King Best Paper Award.

David R. Jackson (S'83–M'84) was born in St. Louis, MO, on March 28, 1957. He obtained the B.S.E.E. and M.S.E.E. degrees from the University of Missouri, Columbia, in 1979 and 1981, respectively, and the Ph.D. degree in electrical engineering from the University of California, Los Angeles, in 1985.

He is currently an Assistant Professor in the Electrical Engineering Department at the University of Houston, Houston, TX. His research interests at present include microstrip and leaky-wave antennas for microwave and millimeter-wave applications.